

NUMERICAL ANALYSIS OF THE STRESS-STRAIN STATE OF A ROPE STRAND WITH LINEAR CONTACT UNDER TENSION AND TORSION LOADING CONDITIONS

Evgenij Kalentev¹, Štefan Václav², Pavol Božek², Valerij Tarasov¹, Alexander Korshunov¹

¹ Institute Mechanics Ural Branch of the Russian Academy of Sciences, T. Baramzina 34, 426067 Izhevsk, Russia, e-mail: eugenedavis@mail.ru; tvv@udman.ru; kai@istu.ru

² Slovak University of Technology, Faculty of Material Science and Technology, J. Bottu 25, 91724 Trnava, Slovak Republic, e-mail: stefan.vaclav@stuba.sk; pavol.bozek@stuba.sk

Received: 2017.04.15
Accepted: 2017.05.07
Published: 2017.06.01

ABSTRACT

The paper presents the results of a numerical analysis of the stress-strain state of a rope strand with linear contact under tension and torsion loading conditions. Calculations are carried out using the ANSYS software package. Different approaches to calculation of the stress-strain state of ropes are reviewed, and their advantages and deficiencies are considered. The analysis of the obtained results leads us to the conclusion that the proposed method can be used in engineering calculations.

Keywords: numerical analysis, stress-strain state, rope.

INTRODUCTION

A steel rope is widely used in modern machinery, particularly in lift-and-carry machines and mechanisms [1, 2]. There are a large number of types of ropes, but the key design factors determinative for structure and applicability of a particular rope type are the following: order of lay, cross section profile of an individual wire, pattern of contact between wires in a strand, contact of wires in a strand [3].

In regular-lay design rope, the wires with helical axis are single or multistage laid around a central straight line wire. The regular-lay ropes are also known as twisted rope. If we continue the laying of a twisted rope, a so-called double-lay rope will be obtained where the twisted rope will be called a strand. It shall be noted that in double-lay ropes the central wire is helical line shaped [4]. Continuing the laying process in a similar manner a rope of any lay order can be obtained. The twisted and double-lay ropes have gained the most widespread currency [5]. If wires are laid into strands in layers with different pitches, the

layers will make contact at points. But if the wire layer pitches are equal, the wires of the upper layer are placed into grooves formed by the wires of the lower layer [6]. In this case the wire layers contact at lines. In strands with a large number of layers the combination of point and line contacts between wire layers is possible [7].

Based on works [8, 9, 10], the analysis of developmental history of a rope concept and its operation affords to distinguish several basic approaches to the calculating theory of ropes and to look through the evolution of these approaches.

Theory of flexible thread, which identifies a rope as a certain superficially equivalent thread with no structural features, prevailed at the beginning of the 1960s and served its purpose of the progress in force analysis of ropes, particularly in problems of mine hoisting dynamics. Dinnik [10] was the first to correlate external elastic properties of rope to its inner geometry.

Glushko [8] and his disciples developed in their works a prospective trend in the mechanics of ropes, which opposed accuracy of calculation and its maximum closeness to the actual con-

struction of rope to the theory of flexible thread. This trend is based on a discrete model: a rope is represented as a complex redundant framework, which is in general calculable by means of structural theory analysis.

An alternative and relatively new trend in the mechanics of ropes is a trend based on continual approach and fundamentally different both from discrete model and the theory of flexible string [9]. The continuous model implies that a rope represents a solid cylinder with anisotropy corresponding to the simulated construction. Within this trend, accuracy of the analytic model (in contrast to the discrete one) improves with the increase in packing density of wires in a rope, while the cross section profile of an individual wire does not matter.

The works [11] and [12], which can be related to the latest research in this field, should be particularly mentioned. The work [11] offers two new approaches, the first of which rests on the theory of fibre composites and the solution of Saint-Venant's problem for cylinder with helical anisotropy. The second approach is based on a finite element solution of three-dimensional problem of elasticity theory for a solid inhomogeneous cylinder formed by a finite number of elastic fibres having a shape of helical lines and joined by weak aggregate (with Young's modulus in several orders lower than Young's modulus of a fibre). The work [12] contains an analysis of fretting damage (mechanical wear of adjoining objects subjected to oscillatory relative microdisplacement), resulting in the reduction of the rope's durability.

Independently of approach employed the relation of axial force T , torque M , axial deformation ε and torsion angle φ is presented in the following analytic form:

$$\begin{aligned} d_{11}\varepsilon + d_{12}\varphi &= T \\ d_{12}\varepsilon + d_{22}\varphi &= M \end{aligned} \tag{1}$$

where d_{11} and d_{22} are generalized coefficients of stiffness under tension and torsion; d_{12} is a certain generalized influence coefficient. It follows that:

- in the general case the axial force, along with axial deformation, creates torsion and the torque, along with torsion, creates axial deformation (the general case is understood here as a situation when one end of the rope is fixed and another one is fully loose),
- the stiffness under tension D_e and torsion D_t essentially depend on the manner of rope ends fixation.

Example 1. Assume that a rope is strained with a force T and its ends are fixed to prevent torsion ($\varphi = 0$). Thereupon having solved the (1) for deformation, we obtain:

$$\begin{aligned} T &= d_{11}\varepsilon, & M &= d_{12}\varepsilon \\ \varepsilon &= \frac{T}{d_{11}}, & M &= \frac{d_{12}}{d_{11}}T \end{aligned} \tag{2}$$

The tension stiffness in this case equals $D_e = d_{11}$. This variant of loading is known as pure tension of a rope. Under the effect of tensile force in the rope the torque occurs, which is balanced with torque in fixation. Obviously, when $\varepsilon = 1$ we obtain $T = d_{11}$ and $M = d_{12}$. Consequently the coefficient d_{11} , equal to the force initiating the unit tensile deformation, represents the stiffness of the rope at pure tension.

Example 2. If the second rope's end is free of fixation preventing the torsion ($\varphi \neq 0$), the rope will untwist under the effect of inner torque. Subsequently we obtain:

$$\varepsilon = \frac{Td_{22}}{d_{11}d_{22} - d_{12}^2}, \quad \varphi = -\frac{Td_{12}}{d_{11}d_{22} - d_{12}^2} \tag{3}$$

This type of loading is commonly referred to as the free tension of a rope. The negative twist means that the rope is untwisting relative to the positive direction of lay. In this case, the torsion stiffness equals to:

$$D_e = \frac{d_{11}d_{22} - d_{12}^2}{d_{22}} \tag{3a}$$

Example 3. Assume that a rope is twisted with torque M , and its ends are fixed to prevent axial displacement ($\varphi = 0$):

$$\begin{aligned} M &= d_{22}\varphi, & T &= d_{12}\varphi \\ \varphi &= \frac{M}{d_{22}}, & T &= \frac{d_{12}}{d_{22}}M \end{aligned} \tag{4}$$

This type of loading is known as pure torsion of a rope. Coefficient d_{22} represents the stiffness of the rope at pure torsion.

As follows from the examples, the influence coefficient d_{12} has two-way mechanical meaning. Under pure tension ($\varepsilon = 1, \varphi = 0$) it equals to torque in the rope, and under pure torsion ($\varepsilon = 0, \varphi = 1$) it equals to axial force.

We shall compare mathematical descriptions for deformation of a twisted rope and deformation of a straight-line elastic solid isotropic rod. The basic difference is that the deformation of the rod under tension and torsion are described by two independent equations [8]:

$$T = EF\varepsilon, \quad M = GI_p\varphi \tag{5}$$

where E - Young's modulus of the material, F - cross-sectional area, I_p - polar second area moment of rod relative to its axis), while we have a system of two equations (1) for a rope. Herewith, all known approaches of elementary theory of straight-line isotropic rods (hypothesis method, Saint-Venant's theory, asymptotic methods of elasticity theory) to a generation of a solution for the problem of the stress-strain state of a rod given the same result for its stiffness under tension: $D_e = d_{11} = EF$. In theory of ropes different approaches lead to different analytic expressions for stiffness d_{ij} [11].

We shall illustrate the application of approaches by Glushko [8], Getman and Ustinov [11] for the calculation of generalized stiffness and influence coefficients. The analytical expressions for generalized stiffness and influence coefficients are as follows:

- according to M. F. Glushko [8]:

$$d_{11} = \sum_i (E_i F_i \cos^3 \alpha_i + E_i I_i \frac{\sin^4 \alpha_i}{r_i^2} \cos^3 \alpha_i + G_i I_{pi} \frac{\sin^6 \alpha_i}{r_i^2} \cos^2 \alpha_i) \tag{6}$$

$$d_{12} = \sum_i (E_i F_i r_i \cos^2 \alpha_i \sin \alpha_i + G_i I_{pi} \frac{\cos^4 \alpha_i}{r_i} \sin^3 \alpha_i - E_i I_i (1 + \cos^2 \alpha_i) \frac{\cos^2 \alpha_i}{r_i} \sin^3 \alpha_i) \tag{7}$$

$$d_{22} = \sum_i (E_i F_i r_i^2 \cos \alpha_i \sin^2 \alpha_i + G_i I_{pi} \cos^7 \alpha_i + E_i I_i (1 + \cos^2 \alpha_i)^2 \sin^2 \alpha_i \cos \alpha_i) \tag{8}$$

- according to [11]:

$$d_{11} = \pi k_1 a^2 E_1 \left[1 - \left(1 + \frac{\nu}{2} \right) \sin^2 \alpha \right] \tag{9}$$

$$d_{12} = \pi k_1 a^3 E_1 \operatorname{tg} \alpha \frac{\left[1 - \left(\frac{4}{3} + \nu \right) \sin^2 \alpha \right]}{2} \tag{10}$$

$$d_{22} = \pi k_1 a^4 E_1 \operatorname{tg}^2 \alpha \frac{\left[1 - \left(\frac{3}{2} + \frac{3\nu}{4} \right) \sin^2 \alpha \right]}{3} \tag{11}$$

In the expressions (6)-(8) the index i is an identifier of a certain wire with E_i - modulus of material's elasticity, F_i - cross-section area, r_i - distance between the rope's axis and the wire's central axis, α_i - lay angle, I_i - second area moment relative to its axis; G_{pi} - shear modulus of the material; I_{pi} - polar second area moment.

The following notations are taken in the expressions (9)-(11): k_1 - parameter, equal to the relation of the total cross-section area of the fibres to the cross-section area of the rope taken as circular cylinder; a - radius of the rope as circular cylinder; E_i - elasticity modulus of the fibre material; α - inclination angle of outer fibre to the rope's axis; ν - Poisson ratio of the fibres.

The benefit of the mentioned approaches is their analytical character. However, to obtain the final formulas, the authors within the problem in hand had to resort to a number of essential simplifications, which are in particular the following:

1. The theory of Academician A.N. Dinnik disregards the transverse contraction of a rope and the stresses due to bending and torsion of the wires. This theory appeared to be inefficient for the assessment of a rope's strength, as it did not provide the actual stress pattern in the rope's cross-section. According to this theory the stresses in the cross-section are uniformly distributed, which contradicts abundant experimental results of analysis of a rope's tensile failure.
2. The theory of M. F. Glushko disregards internal friction forces between the rope's elements. Moreover, the discrete model is not universal. Firstly, as the dimension of the problem directly depends on the number of wires per strand. Secondly, the discrete model provides for point contact of the construction elements.
3. According to the theory of M.F. Glushko, the geometrically equivalent wires or strands in

Table 1. Geometric characteristics of the rope strand wires

No. of Layer	Wires quantity [pcs]	Wires diameter [mm]	Radius of wires' helical axes [mm]	Lay angle [degrees]
0	1	1.8	–	–
1	6	1.7	1.75	10.38
2-1	6	1.4	3.3	19.06
2-2	6	1.8	≈3.059	17.76

each cross-section of the rope are equivalent in force relation as well.

- In work [11] within the finite element analysis of the stress-strain state the contact interaction between the wires are ignored, which leads to the understating of stiffness value d_{II} .

All these factors are taken into consideration in this work, which is dedicated to development of models affording to analyze stress state of rope's strands with linear contact by contemporary numerical methods involving reliable, universal and highly efficient application program packages.

In spite of widespread occurrence of modern software systems and finite elements analysis, the problem of numerical research of rope's stress-strain state is poorly enlightened in Russian scientific literature. The works [12] and [13] can be considered as close to this field. Amongst foreign literature the work [13] could be singled out. Unfortunately, the authors did not succeed in obtaining any additional information, thus the article contains certain descriptive aspects to clarify the matter.

GENERAL DATA ON THE SUBJECT MATTER

The subject of research is a two-lay rope's strand with linear contact of LK-R type and of design 6x19(1+6+6/6)+1 f.c. The rope 25-GL-V-L-O-N-T-1770 GOST 2688-80 (1 f.c. stands for fibre core). The total amount of wires in a strand – 19; wire pitch – 60 mm; strand diameter – 8 mm; lay order – 7,5; length of rope strand $l = 100$ mm; elasticity modulus of the wire material $E = 2 \cdot 10^5$ MPa; Poisson ratio $\nu = 0.3$; friction coefficient $\mu = 0.2$. One of the end faces is firmly fastened (hereinafter the end face of the rope's strand is understood as population of end faces of all wires in the strand). On surface of the opposite end, which is loose, has a simulated rigid behaviour, which most strictly corresponds to real loading conditions of a rope strand. Table 1 presents

some geometric characteristics of wires, which are necessary for rope strand model development.

The research covers cases of static loading of the strand end surface with rigid behaviour. The strand is exposed in turn to axial tensile force T (Variant 1), momentum M initiating torsion of the strand (Variant 2), combination of the force and momentum (Variant 3) (Figure 1). The symmetry conditions are not involved.

The problem of the stress-strain state calculation of a rope strand may be solved as a problem of contact interaction with regard to the friction of geometrically nonlinear wires in spatial stress state.

The objective of the calculation is to define the following characteristics of a rope strand: longitudinal displacement Δl , stress intensity σ_i , movement of wires relative to each other (distance of sliding) s and contact pressures in the wires interaction areas p . The stress-strain state of a rope strand will be obtained by finite element method using ANSYS package.

To create the calculation geometry of the research subject we use one of 3D solid-modelling

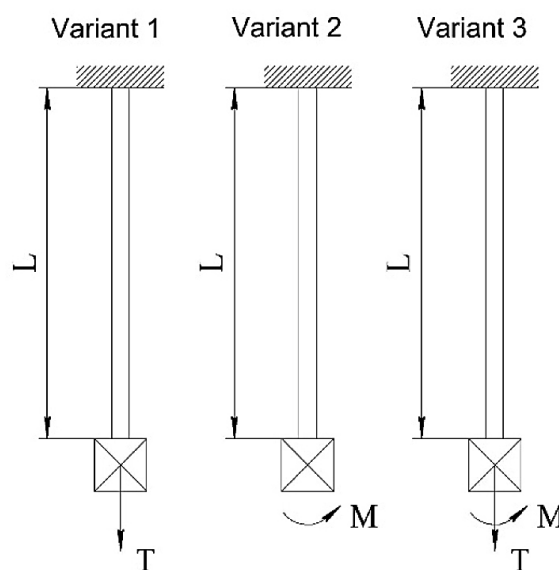


Fig. 1. Analytic models of loading

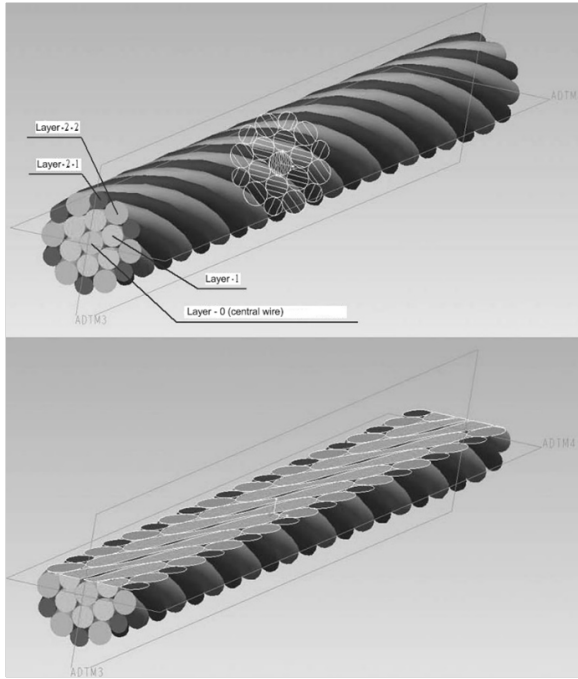


Fig. 2. Calculation geometry of a rope strand with linear contact

systems commonly used in engineering practice. Figure 2 shows the results of rope strand geometry modelling.

The finite element mesh is generated by means of ANSYS built-in operation called “sweep method”. The principle of the method is as follows: one of the wire’s ends is selected as “source”, the other one as “target”, the helical axis of the wire as “path”. The “source” end is divided into finite elements (hexahedrons), which are “protruded” along the “path” up to the “target” end. This procedure is performed for all wires of the rope strand. After this, the length of the finite element edges on the end surface of the rope strand shall be determined. Then to ensure the required accuracy of calculation and structural integrity (regularity) of the mesh, “parametrizing” shall be

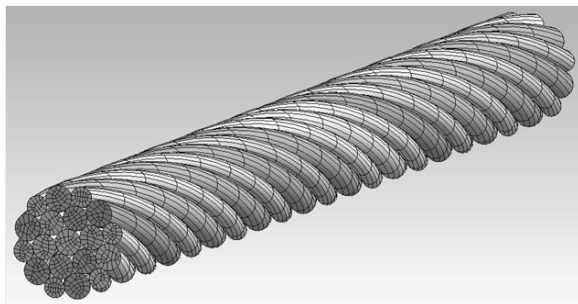


Fig. 3. Finite element model of a rope strand

performed on the lines making up the circumference of each wire end (here “parametrizing” is understood as dividing of the finite elements into requisite number of sections along the selected line in order to develop more detailed mesh). The finite element model generated in this way is presented on Figure 3; the mesh key parameters are listed in the Table 2.

The complicated structure and multiple spatial contact interactions between the rope elements should be referred to basic problems of numerical analysis of linear contact ropes’ stress-strain state (Figure 4). The total amount of contact areas (interfaces) is determined in the following way: the cylindrical surface of each wire is divided into two semi-surfaces – contact and target ones. Consequently, the contacts “Layer 0 – Layer 1” and “Layer 2-1 – Layer 1” involve the whole cylindrical surface of the wires, and in the other cases the contact involves only one of the cylindrical semi-surfaces. Here the contact between the wires is symmetric.

Then from ANSYS package we enter the command RMODIF identifying ICONT parameter, which sets the distance between Gauss point of the contact semi-surface (detection point) and target semi-surface. If the indicated distance is greater than the value of ICONT parameter, the contact is missing (contact with status “open”). Otherwise the surfaces come into contact (the status of contact is “close”). Entering the ICONT parameter affords to decrease discretization degree of the mesh (especially on curved surfaces).

For mathematical description of the contact interactions we employ augmented Lagrange method, which is the basic solution algorithm for such problems in ANSYS 11.0 software package [14, 15]. It rests on the interactive procedure of penalty function method. According to the

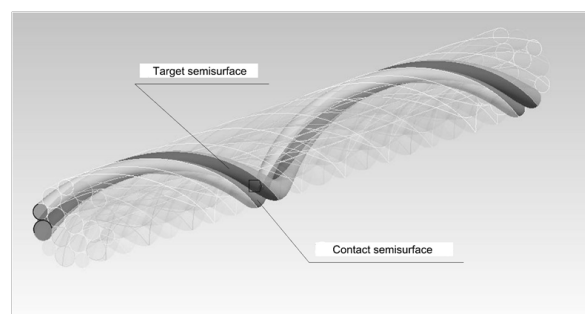


Fig. 4. Wire contact between Layer 2-1 and Layer 2-2 in rope strand

Table 2. Key parameters of finite element mesh

No.	Name of quadratic element	Name in Mechanical APDL	Elements quantity in the rope strand model
1	20-nodal hexahedron	Mesh200	11854
2	8-nodal contact quadrangle	Conta174	9996
3	8-nodal target quadrangle	Targe170	9912

penalty function method, to define the contact area between two surfaces, the concept of contact “spring” is introduced. The stiffness of this “spring” artificially introduced into the algorithm is called contact stiffness k and is a parameter of penalty function. If the status of a contact is “open”, which means that the surfaces have not come into contact, the “spring” is disabled, and when the surfaces come to into contact the “spring” becomes engaged and involved in the calculation algorithm. The “spring” is stretched by the value Δ , and the equilibrium occurs in the contact area as the value of contact force $F = k\Delta$ becomes equal to the value of external loading. To ensure the balance of internal and external forces the value Δ shall be greater than zero. In reality, interpenetration of two contact surfaces does not occur, but in ANSYS interpenetration is artificially introduced for the successful generation of a contact pair. The basic contact parameters (contact pressure and friction stress) are increasing during the additional iterating process so that the ultimate penetration is less than the prescribed value of penetration allowance. The advantages of augmented Lagrange method include the facts that the algorithm on its basis minimizes the in-

terpenetration of the two contact surfaces and has less sensitivity towards value of contact stiffness, has better convergence conditions in comparison with immediate penalty function method [14].

STRESS-STRAIN STATE OF A STRAND UNDER VARIOUS LOADING CONDITIONS

Let us consider some results of the research. Table 3 presents data obtained in the separate layers of the rope strand, and Figures 5-7 illustrate axial deformation and stress intensity distribution within the rope strand in general under various loading conditions.

To estimate the accuracy of the obtained results we compare them with results of calculation by other authors’ approaches (see [8] and [11]). For this purpose, we will solve the equation (1) for deformation:

$$\begin{aligned} \varepsilon &= \frac{Td_{22}}{d_{11}d_{22} - d_{12}^2} - \frac{Md_{12}}{d_{11}d_{22} - d_{12}^2} \\ \varphi &= -\frac{Td_{12}}{d_{11}d_{22} - d_{12}^2} + \frac{Md_{11}}{d_{11}d_{22} - d_{12}^2} \end{aligned} \tag{12}$$

Table 3. Basic calculation results of stress-strain state of a rope strand

No. of loading variant	Loading values	Wire layers	Longitudinal displacements Δ [mm]	Stress intensity σ_{ekb} [MPa]	Contact pressure p [MPa]	Distance of sliding $S \cdot 10^{-3}$ [mm]
1	T=1000 H M=0	0	0.034	58–80	0.3	1.4
		1	0.034	21–90	0.39	1.2
		2–1	0.034	12–121	4.8	1.5
		2–2	0.034	10–87	6.8	1.8
2	T=0 M=1 Hm	0	-0.041	70–84	0	0
		1	-0.041	14–78	0.6	0.7
		2–1	-0.041	10–97	0.5	1.2
		2–2	-0.041	5–66	7.0	1.5
3	T=1000 H M=1 Hm	0	0.008	14–20	0.5	0.7
		1	0.008	12–30	0.6	1.4
		2–1	0.008	28–70	5.1	1.6
		2–2	0.008	12–33	6.8	2.1

Then using the formulas (6)÷(8) and (9)÷(11) we determine the coefficients of stiffness and influence. Taking into account that $\epsilon = \Delta l/l$ we shall find the longitudinal displacements Δl for different variants of loading:

$$\Delta l = \frac{Td_{22}}{d_{11}d_{22} - d_{12}^2}l \quad (13)$$

$$\Delta l = -\frac{Md_{12}}{d_{11}d_{22} - d_{12}^2}l \quad (14)$$

$$\Delta l = \left(\frac{Td_{22}}{d_{11}d_{22} - d_{12}^2} - \frac{Md_{12}}{d_{11}d_{22} - d_{12}^2} \right)l \quad (15)$$

The calculation results are summarized in Table 4. As we can see in the table, the authors' solution in terms of results is closer to the approach of Glushko M. F., which currently is the maximum proximate to the real construction of ropes. The significant disagreement with results of I. P. Getman, Yu. A. Ustinov is explained by the sufficiently large difference in values of coefficients of stiffness d_{22} and influence d_{12} , which is caused by an absence of internal relations between individual fibres (this issue is exhaustively covered in work [11]). However the calculations of stiffness coefficient d_{11} by methods [8] and [11] as well as by the authors' solution give results with spread within 3%. The authors have succeeded in obtaining results, which align with results of the work [9] in a qualitative sense only, thus the comparison with this method has not been brought here. It should be mentioned that the approaches [8] and [11] do not enable to define the distances of sliding.

Let us analyse the rope strand behaviour in general and under different variants of loading.

Variant 1. The stress-strain state of a rope strand as longitudinal tensile force is applied (Figure 5).

This type of loading results in elongation of the rope strand in direction of the force action

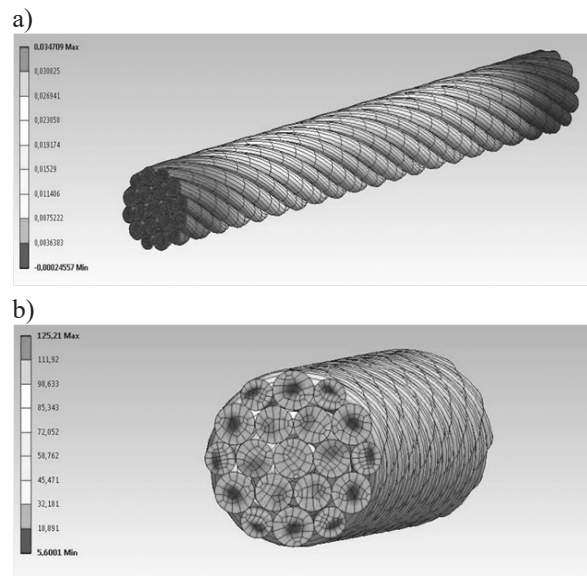


Fig. 5. Axial deformation (a) and distribution of stress intensity (b) as longitudinal tensile force is applied to a rope strand

(Figure 5a) attended with untwisting. The intensity of stresses is of a non-uniform nature. Thus in the central wire the stresses are uniformly distributed over its cross-section, in wires of the second layer the stress minima are focused in the centre while the maxima are localized in the areas of contact with the adjoining wire layer (the 1st layer) and in contact areas between wires in the layer itself (Figure 5b).

Variant 2. The stress-strain state of a rope strand as a torsion moment is applied (Figure 6).

At the second variant of loading the rope strand is intertwisting, the wire lay angles are increasing, the strand is contracting, which is attended with its shrinking (shortening) (Figure 6a). The stress intensities are distributed non-uniformly (Figure 6b); in the central wire due to its twisting, the stress rises progressively as approaching the wire's outer surface. In wires of the first layer there are local maxima in areas of

Table 4. Longitudinal displacements Δl in a rope strand calculated by different methods

No. of loading variant	Loading values	Longitudinal displacements Δl [mm]		
		Method by M.F. Glushko [2]	Method by I.P.Getman, Yu.A. Ustinov [4]	The authors' solution
1	T=1000 H M=0	0.0340	0.077	0.034
2	T=0 M=1 Hm	-0.0300	-0.098	-0.041
3	T=1000 H M=1 Hm	0.0048	-0.021	0.008

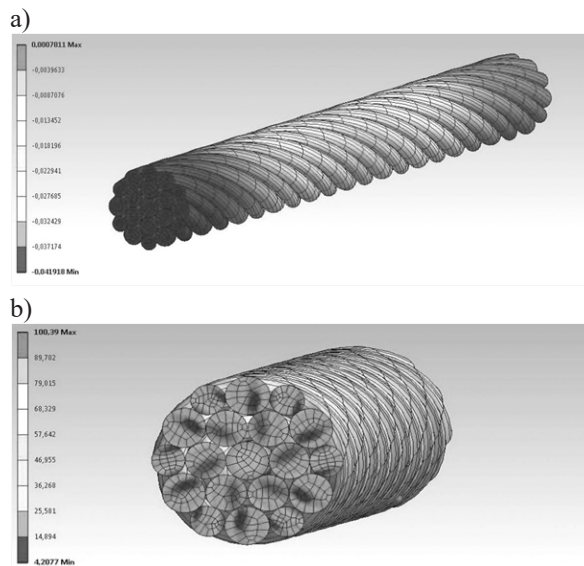


Fig. 6. Axial deformation (a) and distribution of stress intensity (b) as a torsion moment is applied to a rope strand

contact interaction with the neighbouring wires; in the outer layer the maxima of stress intensity are displaced towards contact areas of the wires in the layer itself.

Variant 3. The stress-strain state of a rope strand as longitudinal tensile force and a torsion moment are applied.

Under the complex loading the absolute value of the strand elongation is small in comparison with the other loading variants, which can be explained by a combination of the loads: the tensile force tends to stretch the rope strand, while the torsion moment on the contrary tends to shrink it (Figure 7a). As in previous cases, the stress intensities are distributed non-uniformly (Figure 7b). However, the spread is not so great in the central wire and in the wires of the first layer. The layer 2-1 exhibits maxima of stress intensities in areas of contact with the 1st layer wires.

In all three cases, the maximum contact stresses can be observed in wires of the outer layer and the distances of sliding are disturbed uniformly along the wire length (see Table 3). The work [14] shows that the major factors responsible for fretting caused by contact interaction are the contact pressures and sliding speed. The sliding speed can be determined through distances of sliding and the duration of load application. This enables us to define the scientific based fretting law, which is the law of wire dimension variations in direction of axis perpendicular to the friction sur-

face, as a consequence of their deformation in the friction process. In the future, this will enable an approach to the problem of methods developed for the analysis on ropes durability.

On the whole, the behaviour of the rope strand model agrees well with the equations (1). The occurrence of significant contact pressures and sliding of the wires relative to each other gives the reason to assume that they contribute significantly to the performance of a rope in general and call for further investigation.

CONCLUSIONS

Considered in this work, the numerical analysis method affords to investigate behaviour of a rope strand with linear contact of wires under various loading conditions, to determine the contact interactions between the wires, and can be used as an auxiliary tool in engineering applications. Thus, this method enables us to:

- provide recommendations on the usage of a particular lubricant. For this purpose the contact algorithm of ANSYS package requires introduction of values of friction coefficient between rope strand wires, which were obtained from experiments with various lubricants, further calculation and comparison of the corresponding stress-strain states;
- approach more soundly the issue of ropes cull (by simulating breakage of one or more wires

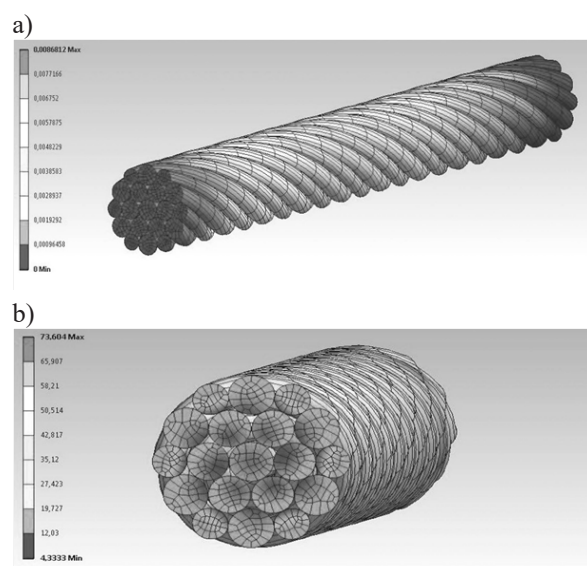


Fig. 7. Axial deformation (a) and distribution of stress intensity (b) as longitudinal tensile force and a torsion moment are applied to a rope strand

and estimating redistribution of stresses and deformation);

- numerically analyse the stress-strain state of ropes with more complicated design (irregular-laid ropes and so called locked or semi-locked ropes) by creating the non-circular cross-section of wires.

Acknowledgements

This work is a part of project KEGA 014STU-4/2015. The article was supported by the VEGA 1/0477/14 project “Research of influence of selected characteristics of machining process on achieved quality of machined surface and problem free assembly using high Technologies” supported by the scientific grant agency of the Ministry of Education of the Slovak Republic and of Slovak Academy of Sciences. This publication is the result of implementation of the project: “University Scientific Park: Campus MTF STU - CAMBO” (ITMS: 26220220179) supported by the Research & Development Operational Program funded by the EFRR.

REFERENCES

1. Peterka P., Krešák J., Kropuch S., Fedorko G., Molnar V. and Vojtko M. Failure analysis of hoisting steel wire rope. *Eng. Fail. Anal.*, 45, 2014, 96–105.
2. Gajdos I., Slota J., Spisak E., Jachowicz T. and Tor-Swiatek A. Structure and tensile properties evaluation of samples produced by Fused Deposition Modeling. *Open Engineering* 2016, 6 (1), 86–89.
3. Molnár V., Boroška J. and Dečmanová J. Mechanical properties of steel rope wires — quality test assurance. *Acta Montan. Slovaca*, 15, 2010, 23–30.
4. Stanova E., Fedorko G., Kmet S., Molnar V. and Fabian M. Finite element analysis of spiral strands with different shapes subjected to axial loads. *Adv. Eng. Softw.*, 83, 2015, 45–58.
5. Madáč K., Durkáč V. and Král' J. Design of applications for CAD system Creo Parametric 1.0. *Int. Sci. Her.*, 4, 2012, 278–284.
6. Debski H., Koszalka G. and Ferdynus M. Application of FEM in the analysis of the structure of a trailer supporting frame with variable operation parameters. *Ekspluat. i Niezawodn. – Maint. Reliab.*, 14, 2012, 107–113.
7. Kmet S., Stanova E., Fedorko G., Fabian M. and Brodniansky J. Experimental investigation and finite element analysis of a four-layered spiral strand bent over a curved support. *Eng. Struct.*, 57, 2013, 475–483.
8. Glushko M.F. *Steel wire hoisting ropes*. Technika, Kiev, 1966.
9. Musalimov V.M. *Mechanics of Deformable Cable*, St. Petersburg, 2005.
10. Dinnik A.N. *Mining engineering articles*. Ugletekhizdat, Moscow, 1966.
11. Getman I.P. and Ustinov Y.A. Concerning methods of ropes analysis. *Strain-torsion problem*, 2008, 81–90.
12. Taltykin V.S. Method validation for improvement of mining ropes durability with regard to contact interaction of wires, (2009).
13. Erdönmez C. and İmrak C.E. Modeling and numerical analysis of the wire strand. *J. Nav. Sci. Eng.*, 5, 2009, 30–38.
14. Goryacheva I.G. and Dobychin M.N. *Contact problems in tribology*. Engineering, Moscow, 1988.
15. Božek P. and Pivarčiová E. Flexible manufacturing system with automatic control of product quality, *Strojarnstvo*, 55(3), 2013, 211-221.